MEK and Cdc2 Kinase Are Sequentially Required for Golgi Disassembly in MDCK Cells by the Mitotic *Xenopus* Extracts

Fumi Kano,*‡‖ Katsuya Takenaka,‡ Akitsugu Yamamoto,§ Kuniaki Nagayama,* Eisuke Nishida,‡ and Masayuki Murata*‖

*Department of Molecular Physiology, National Institute for Physiological Sciences, Okazaki 444-8585, Japan; ‡Department of Biophysics, Graduate School of Science, Kyoto University, Kitashirakawa, Sakyo-Ku, Kyoto 606-8502, Japan; §Department of Physiology, Kansai Medical University, Osaka 570-8506, Japan; and ‖CREST, Japan Science and Technology Corporation, Japan

Abstract. At the onset of mitosis, the Golgi apparatus, which consists of several cisternae, disperses throughout the cell to be partitioned into daughter cells. The molecular mechanisms of this process are now beginning to be understood. To investigate the biochemical requirements and kinetics of mitotic Golgi membrane dynamics in polarized cells, we have reconstituted the disassembly of the Golgi apparatus by introducing *Xenopus* egg extracts into permeabilized Mardin-Darby canine kidney (MDCK) cells. We used green fluorescence protein (GFP)-tagged galactosyltransferase-expressing MDCK cells to analyze the morphological changes of the Golgi membrane in the semi-intact system. Analyses by fluorescence and electron microscopies showed that the Golgi disassembly can be dissected into two elementary processes morphologically. In the first process, the perinuclear Golgi stacks break into punctate structures, intermediates, which are comprised of mini-stacks of cisternae associating with apical microtubule networks. In the second process, the structures fragment more thoroughly or substantially relocate to the ER. Our analyses further showed that cdc2 kinase and mitogen-activated protein kinase kinase (MAPKK = MEK) are differently involved in these two processes: the first process is mainly regulated by MEK and the second mainly by cdc2.

Key words: Golgi complex • mitosis • semi-intact cells • GFP • kinase

Introduction

Recent advances in green fluorescence protein (GFP)[1] tagging of organelles allow us to observe the dynamic structural changes of the Golgi apparatus as well as those of the nucleus or ER membranes in living mammalian cells during mitosis (Ellenberg et al., 1997). Shima et al. (1997, 1998) reported that in mitotic phase the Golgi apparatus first reorganizes into 1–3-μm fragments, which subsequently fragment and disperse into smaller vesicles from metaphase to anaphase, and that the position of mitotic Golgi fragments correlates with the mitotic spindle. These observations suggest that the position and dynamics of mitotic Golgi fragments are regulated actively during mitosis contrary to the passive diffusion model (Warren and Wickner, 1996). Most recently, Zaal et al. (1999) proposed that during mitosis absorption of the Golgi membranes into the ER, instead of thorough fragmentation and dispersion of the fragments, takes place. In their model, the perinuclear Golgi ribbon structures are lost at prophase and peripheral Golgi fragments appear; the fragments are tubular-membrane clusters (0.5–2.0-μm-diam) that scatter throughout the cytoplasm. Then, the clusters are lost and Golgi proteins are redistributed into the ER. Their model was based on their findings that in mitotic phase the export from the ER is inhibited while the retrograde traffic of Golgi proteins is not, and consequently the proteins come to reside primarily within ER instead of isolated Golgi-derived vesicles or fragments. Thus, through morphological analyses in living cells, the molecular mecha-

Address correspondence to Masayuki Murata, Department of Molecular Physiology, National Institute for Physiological Sciences, Okazaki 444-8585, Japan. Tel.: 181-564-55-7815. Fax: 181-564-52-7913. E-mail: mmurata@nips.ac.jp

The present address of Katsuya Takenaka is Department of Cell Biology, Max-Planck-Institute for Biochemistry, Am Klopferspitz, 18a, D-82152 Martinsried, Germany.

[1]*Abbreviations used in this paper:* BL, butyrolacotone I; ERK, extracellular signal-regulated kinase; GT-GFP, GFP-tagged mouse galactosyltransferase; GFP, green fluorescence protein; IC, Cdc2-activated interphase extracts; IS, MEK-activated interphase extracts; ISC, cdc2-activated interphase extracts; M, mitotic; MEK, mitogen-activated protein kinase kinase; NRK, normal rat kidney; PD, PD98059; PDI, protein disulfide isomerase; r.t., room temperature; SB, SB203580; SLO, streptolysin O; SS, staurosporine; TB, transport buffer; TEM, transmission electron microscopy; TRITC-phalloidin, tetramethylrhodamine B isothiocyanate–labeled phalloidin.

nisms of mitotic Golgi disassembly are beginning to be understood.

Many mitotic events are believed to be regulated by protein kinases. Cdc2, which is a master regulator of mitotic phase entry, plays a crucial role in chromosome condensation, mitotic spindle formation, and disassembly of the nuclear lamina (Nigg, 1995). Cdc2 activation was also shown to inhibit transport between Golgi cisternae (Mackay et al., 1993; Stuart et al., 1993). Recent studies have suggested that the MEK (mitogen-activated protein kinase kinase)-1/ERK (extracellular signal-regulated kinase) pathway also participates in mitotic events. MEK is a specific activator of ERK1 and 2, which function as essential regulators of cell growth and differentiation in eukaryotic cells (Nishida and Gotoh, 1993). In cycling *Xenopus* egg extracts, MAP kinase activation is essential for maintenance of the mitotic state (Guadagno and Ferrell, 1998). There have also been reports suggesting the involvement of MEK in mitotic phase progression (Bitangcol et al., 1998; Chau and Shibuya, 1998). These findings suggest that the MEK/ERK pathway is an important regulator during mitosis in *Xenopus* egg extracts.

Several recent studies examined requirements of these protein kinases for mitotic Golgi disassembly in mammalian cells. Acharya et al. (1998) reported the Golgi disassembly in vitro in digitonin-permeabilized normal rat kidney (NRK) cells by adding a mammalian mitotic phase cytosol. By using this in vitro system, they showed evidence that MEK, which might lie downstream of cdc2 in a kinase cascade, activates unknown target molecules retained in the permeabilized cells to bring about Golgi disassembly. By contrast, Misteli and Warren (1994) and Lowe et al. (1998) report that cdc2 itself is a Golgi fragmentation kinase. Based upon electron microscopical observation, they studied mitotic Golgi fragmentation in a cell-free system by incubating purified Golgi membranes with cytosol prepared from mitotic HeLa cells, and showed that inhibition of cdc2 kinase function in vitro blocks the Golgi fragmentation.

To investigate the biochemical requirements and kinetics of Golgi membrane dynamics during mitosis, we have reconstituted the disassembly of the Golgi apparatus visualized by GFP-tagged proteins by adding *Xenopus* egg extracts to permeabilized MDCK cells. We have used a morphometric analysis to monitor morphological changes of the Golgi apparatus in this semi-intact cell system. To this end, we produced the stable transfectant MDCK-GT, which continuously expresses mouse galactosyltransferase (GT) fused with GFP (GT-GFP). MDCK-GT cells were permeabilized by treatment with a bacterial pore forming toxin, streptolysin O (SLO), and depleted of most of the cytosol. Then the permeabilized cells were incubated with the *Xenopus* egg mitotic (M) phase extracts in the presence of an ATP-regenerating system. Under the conditions, we were able to reproduce the mitotic Golgi disassembly. By using this system, we have shown that the Golgi disassembly process consists of two steps. First, the stacks of Golgi cisternae fragment into smaller punctate structures associating with the apical network of microtubules. Second, these punctate structures vesiculate into small vesicles or relocate into the ER. We have also studied the kinetics of disassembly and the protein kinases required for each step and found that both cdc2 and MEK in *Xenopus* egg extracts are responsible for the Golgi disassembly. Both protein kinases have overlapping functions, but the first step is mainly regulated by MEK and the second step by cdc2.

Materials and Methods

Cell Culture

MDCK cells were maintained in MEM (Nissui) supplemented with 10% fetal bovine serum (JRH Biosciences), 100 U/ml penicillin G, 100 μg/ml streptomycin, and 0.25 μg/ml fungizone at 37°C in a 5% CO_2 incubator. MDCK cells were cultured on 60-mm tissue culture dishes (Nunc Inc.), and were subcultured to 2.0×10^5 cells every 3 d. MDCK-GT, a MDCK cell line stably expressing mouse galactosyltransferase-GFP, were maintained similarly in complete medium with 300 μg/ml GENETICIN (GIBCO BRL).

Antibodies and Reagents

The following antibodies were used: rabbit anti-MEK polyclonal antiserum as described in Kosako et al. (1994), rabbit antiserum against rat protein disulfide isomerase (PDI) as described in Akagi et al. (1988), mouse anti-cdc2 monoclonal antibodies (Santa Cruz Biotechnology), mouse anti–α-tubulin monoclonal antibody (Sigma), mouse anti-GM130 antibody (Transduction Laboratories), FluoroLink™ Cy™3–labeled goat anti–mouse IgG (H+L) (Amersham International), and Texas red–labeled goat anti–rabbit IgG (H+L) (Vector Laboratories, Inc.). SLO was purchased from Dr. Sucharit Bhakdi (University of Meintz, Germany). PD98059 was purchased from New England Biolabs, Inc. and stored as 50 mg/ml stock in DMSO. Butyrolactone I (Affiniti Research Products), SB 203580 (Calbiochem), and staurosporine (WAKO Pure Chemicals) were stored at 100, 20, and 25 mg/ml in DMSO, respectively. U0126 was purchased from Promega. ATP (adenosine 5′-triphosphate) and creatine kinase (all Sigma) were stored as 100- and 800-mM stock in water. Creatine kinase (Sigma) was prepared as 5-mg/ml stock in 50% glycerol. Chymostatin and pepstatin A (Sigma) were stored as 5-mg/ml stock in DMSO. Leupeptin and antipain (Sigma) were prepared as 5-mg/ml stock in water.

DNA Constructs and Transfection

Complementary DNA encoding 1–60 amino acids of mouse galactosyltransferase was amplified from a mouse liver cDNA library by polymerase chain reaction methods. Primers were 5′-GGCCTGCAGGCATATTCCCAAAACACGA-3′ and 5′-GGCGCTAGCTTGCTTGCCTGGACCTAAGATTTTC-3′. The PCR fragment was inserted in-frame upstream of EGFP cDNA in EGFP-N1 vector (Clontech). In the preparation of human *N*-acetylglucosaminyltransferase I (NAGT) fused with GFP, cDNA encoding 1–103 amino acids of NAGT was amplified and placed upstream of EGFP cDNA in EGFP-N3 vector (Clontech). Primers were 5′-GCCTCGAGGGATGCTGAAGAAGCAGTCTG-3′ and 5′-TCACAGGCGATGACCAGGATGGGAATCAC-3′ (Shima et al., 1998). PCR fragments and EGFP-N3 vector were digested by XhoI-Cfr10I and XhoI-XmaI, respectively. The PCR fragments and vectors were ligated by DNA ligation kit ver. 2 (TaKaRa). MDCK cells were transfected by LipofectAMINE PLUS (GIBCO BRL) according to the instructions. Stable transfectants were selected in complete medium containing 300 μg/ml GENETICIN. After 10 d, surviving cell colonies were isolated and screened visually for Golgi-localized fluorescence. Several positive clones were identified and expanded into cell lines for further experiments.

Preparation of Xenopus Egg Extracts and Kinase Assays

Xenopus egg extracts were prepared essentially according to the method described by Murray (1991), except that cytochalasin B was omitted. The extracts were diluted sevenfold with transport buffer (TB; 25 mM Hepes-KOH (pH 7.4), 115 mM potassium acetate, 2.5 mM $MgCl_2$, 1 mM DTT, and 2 mM EGTA) containing protease inhibitors (25 μg/ml of chymostatin, pepstatin A, leupeptin, and antipain) and centrifuged by Optima™ TLX (Beckman Instruments Inc.) at 42,000 rpm for 60 min at 4°C using a TLA 45 rotor. The supernatant was collected and stored at −80°C. Kinase

activities toward histone H1 and MBP were assayed as described by Takenaka et al. (1997).

Golgi Disassembly Assay

MDCK-GT cells were grown on the polycarbonate membrane (Transwell™; Corning Costar) and incubated with 5 μg/ml taxol (Sigma) for 30 min at 37°C to stabilize microtubules. Cells were treated with 0.1 ml of 500 ng/ml preactivated SLO for 20 min at 4°C. After washing out excess SLO twice with ice-cold PBS, the cells were incubated with pre-warmed TB for 20 min at 37°C to form pores in plasma membranes. The permeabilized cells were incubated in 1 M KCl in TB for 5 min at 4°C to remove peripheral membrane proteins. 60% of total cytosol was leaked under these conditions, which were determined by measurement of cytosolic lactate dehydrogenase leakage (Schnaar et al., 1978). To determine the efficiency and extent of SLO-mediated permeabilization, we tested the accessibility of exogenously added TRITC-phalloidin, a small bicyclic peptide that binds with high affinity to actin filaments (Barak et al., 1980). No staining of actin with TRITC-phalloidin was observed in intact MDCK-GT cells, but the semi-intact cells prepared by SLO treatment exhibited staining of actin filaments demonstrating that small molecules such as TRITC-phalloidin (1.2 kD) could access the semi-intact cells. Under the same conditions, staining of microtubules with anti–α-tubulin antibody (IgG) was also observed in semi-intact cells. Although >95% of filter grown cells were found to be permeabilized by SLO treatment, the intensity of staining varied slightly from cell to cell, suggesting that some cells had more or larger holes than others. However, the variations in the efficiency and extent of permeabilization were too small to affect the quantitative assays by morphometric analysis described below. After these treatments, the polycarbonate membranes were cut into 10 6-mm^2 fragments. The fragments were incubated with 20 μl of reaction mixture for an appropriate time at 33°C. The reaction mixture contained *Xenopus* egg extracts, ATP regenerating system (1 mM ATP, 8 mM creatine kinase, and 50 μg/ml creatine phosphate), 1 mg/ml glucose, and 1 μg/ml TRITC-phalloidin. TRITC-phalloidin was added to all reaction mixtures to check the extent of permeabilization in brief. After incubation, the cells were fixed with 1% formaldehyde in TB for 20 min at room temperature. Samples were observed by an Axiovert 135 fluorescence microscope (Carl Zeiss Inc.) equipped with a color chilled 3CCD camera (model C5810: Hamamatsu Photonics) using a ×63 Zeiss Planapo lens (NA1.4) or LSM 510 confocal microscope system (Carl Zeiss Inc.).

Morphometric Analysis

The disassembly could be classified into three stages based on fluorescence microscopic observation: stage I (intact), a perinuclear, tubular cisternae around the nucleus; stage II (punctate), punctate membranous structures, which were smaller than the intact tubular cisternae; stage III (dispersed), completely dispersed profiles of Golgi membranes. The morphological properties of Golgi membranes at each stage were easily distinguished by a fluorescence microscopy. After appropriate treatments, cells were fixed with 1% formaldehyde in TB and observed with a fluorescence microscope. On triplet coverslips, cells were counted in three hundreds in random fields in each sample. Three independent experiments were performed and means and standard deviations of the number of cells at stage I, II, and III were calculated. Morphological changes of Golgi membranes were expressed as the percentage of cells at stage I, II, and III, respectively.

Fluorescence and Electron Microscopic Observation

After appropriate treatments, semi-intact cells grown on the polycarbonate membranes or glass coverslips were fixed with acetone and methanol solution (mixed at equal volume and stored at −20°C) at 4°C for 6.5 min or with 3% paraformaldehyde at room temperature (r.t.) for 30 min. In the case of paraformaldehyde fixation, cells were permeabilized with 0.2% Triton X-100 at (r.t.) for 20 min. The cells were incubated with 5% skim milk in TB at r.t. for 30 min. And then the cells were incubated with first antibodies (mouse anti–α-tubulin monoclonal antibody, rabbit anti-PDI polyclonal antibody or mouse anti-GM130 antibody) at r.t. for 2 h, and with second antibodies (FluoroLink™ Cy™3–labeled goat anti–mouse IgG (H+L)) at r.t. for 1 h. The specimens were mounted on the slide glasses and viewed with a confocal or fluorescence microscope. For electron microscopic observation, samples were fixed and processed according to protocol 6 described by Hughson and Hirt (1996).

Immunodepletion

Diluted *Xenopus* egg extracts (150 μl, 4.5–5.5-mg/ml protein concentration) were incubated with antibody-coupled beads (20 μg anti-cdc2 antibodies on 30 ml of protein A–Sepharose (or 30 μl of anti-MEK antiserum on 30 μl of protein G–Sepharose; Amersham Pharmacia Biotech) for 1 h at 4°C. The beads were removed by centrifugation and another 30 μl of antibody-coupled beads was added for an additional 1 h at 4°C. This treatment was repeated twice in preparation of cdc2-depleted extracts. The beads were removed and the supernatants were stored at −80°C. The extent of depletion was confirmed by SDS-PAGE and immunoblotting using mouse anti-cdc2 monoclonal antibodies or rabbit anti-MEK antiserum.

Results

The Golgi Disassembly Induced by Xenopus Egg Extracts in Semi-intact MDCK-GT Cells

To investigate the disassembly of Golgi membranes induced by *Xenopus* egg extracts in semi-intact MDCK cells, we used the GT-GFP as a fluorescence probe, which has been used in the study of Golgi membrane dynamics in living cells and characterized in detail (Cole et al., 1996). The stable transfectant, MDCK-GT, which continuously expressed GT-GFP, was cloned and used for the subsequent experiments. MDCK-GT cells, grown on polycarbonate membranes, were preincubated with 5 μg/ml taxol in culture medium for 30 min at 37°C to stabilize microtubules. The cells were then permeabilized by the two-step SLO treatment (see Materials and Methods). In our experiments, SLO was usually added from the apical side of the epithelial sheet of MDCK-GT cells. Then semi-intact MDCK-GT cells were incubated with 1 M KCl in TB for 5 min at 4°C to remove peripheral membrane proteins. The salt wash was essential for the Golgi disassembly by *Xenopus* egg (M phase) extracts. Then cells were incubated with either the ATP regenerating system (hereafter referred to as ATP) only, *Xenopus* egg extracts (protein concentration 5.0 mg/ml) and ATP, or *Xenopus* interphase extracts (at the same protein concentration as *Xenopus* egg extracts) and ATP, respectively, for 60 min at 33°C. All reaction mixtures contained 1 mg/ml glucose and 1 μg/ml TRITC-phalloidin. After incubation, the cells were fixed and viewed under a confocal microscope.

As shown in Fig. 1 A, perinuclear, tubular structures of the Golgi apparatus were observed in semi-intact cells incubated only with ATP. It was a typical construction of the Golgi apparatus in the MDCK-GT cells which formed an epithelial sheet on polycarbonate membranes. Incubation with *Xenopus* interphase extracts did not affect the Golgi structure significantly, although the Golgi cisternae appeared to be less clustered (Fig. 1 C). By contrast, incubation with *Xenopus* egg (M phase) extracts caused the disassembly of Golgi and the fluorescence of GT-GFP was completely diffused throughout the cytoplasm (Fig. 1 B). The characteristic diffused staining pattern of GT-GFP, which contained small heterogeneous vesicular structures, was seen as typical of Golgi membranes in mitotic living MDCK-GT cells (Fig. 3 A, last panel).

To ascertain that the lipid and other Golgi proteins except GT-GFP were relocated during the disassembly, we performed indirect immunofluorescence with an anti-GM130 monoclonal antibody. GM130 is a cis-Golgi matrix

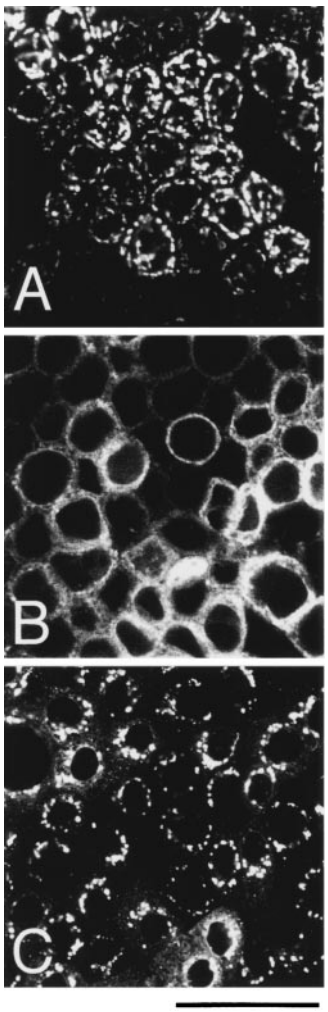

Figure 1. The Golgi disassembly induced by *Xenopus* egg extracts. MDCK-GT cells, grown on polycarbonate membrane, were pretreated with 5 mg/ml taxol at 37°C for 30 min. The cells were permeabilized by SLO treatment and washed with 1 M KCl. Then they were incubated with either ATP (A), *Xenopus* egg extracts and ATP (B), or *Xenopus* interphase extracts and ATP (C), respectively, at 33°C for 60 min. After incubation, the cells were fixed and viewed by confocal microscope. A typical perinuclear structure of the Golgi in MDCK-GT cells was observed (A). *Xenopus* egg extracts and ATP caused mitotic Golgi disassembly (B). *Xenopus* interphase extracts did not affect the Golgi structures, although some loosening of the stacking was observed (C). Bar, 50 μm.

protein (Nakamura et al., 1995). After being treated with *Xenopus* egg extracts and ATP, a dispersed staining pattern of GM130 was observed (data not shown). A significant overlap in the distribution of GT-GFP and GM130 in both intact- and dispersed-Golgi membranes was observed, although there was a subtle difference in staining pattern which may reflect differences in localization of the two proteins in Golgi membranes. We also examined another GFP-tagged Golgi resident protein. MDCK cells, which transiently expressed the human *N*-acetylglucosaminyltransferase fused with GFP (NAGT-GFP), were permeabilized and incubated with *Xenopus* egg extracts and ATP. As a result, a dispersion of NAGT-GFP occurred. In addition, the dispersion of Golgi apparatus in this system was also detected by BODIPY-ceramide, which is a lipid marker of Golgi membranes (data not shown).

Thus, it is likely that *Xenopus* egg (M phase) extracts are able to induce the Golgi disassembly in semi-intact MDCK-GT cells, which is observed in the mitotic Golgi apparatus in living cells.

Time Course of the Golgi Disassembly in Semi-intact Cells

To study the time course of Golgi disassembly, semi-intact, salt-washed MDCK-GT cells were incubated with *Xenopus* egg extracts at 33°C (Fig. 2). 20–40 min after incubation with *Xenopus* egg extracts, perinuclear Golgi stacks were disorganized into numerous punctate structures. After 60 min incubation, the Golgi punctate structures disap-

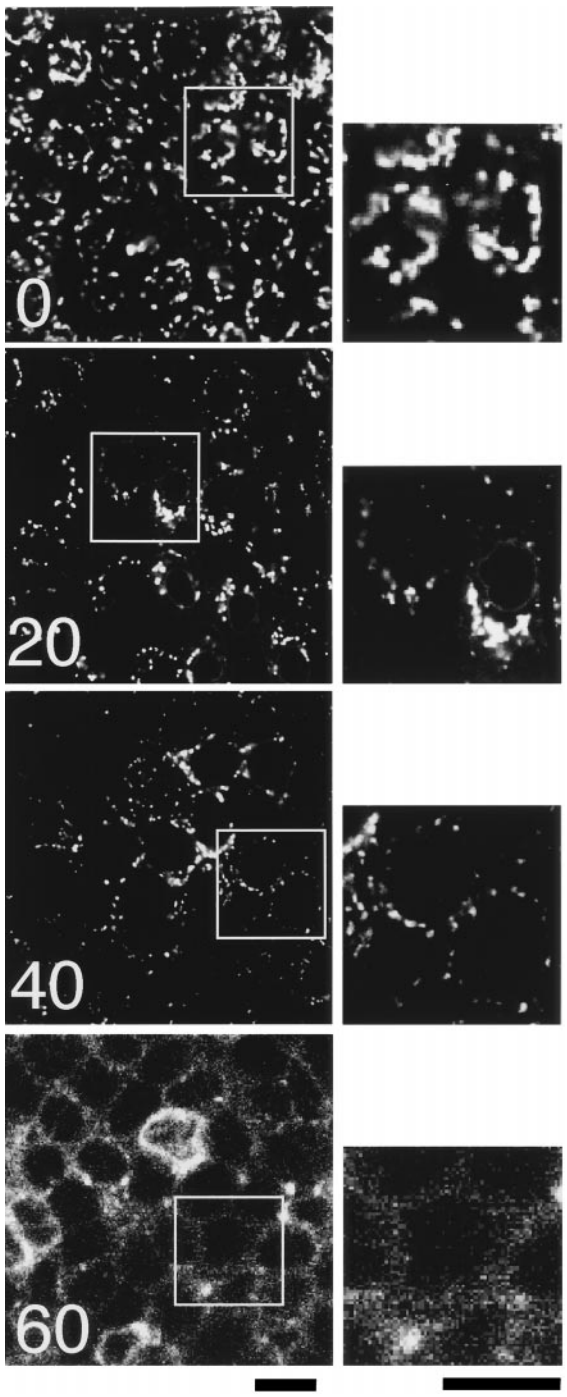

Figure 2. Time course of the Golgi disassembly induced by *Xenopus* egg extracts. Semi-intact MDCK-GT cells were incubated in the presence of the extracts and ATP at 33°C for 0, 20, 40, and 60 min, and then fixed and viewed by confocal microscope. Perinuclear cisternae disorganized into punctate structures during 20–40 min incubation. The Golgi membranes appeared to be dispersed throughout the cytoplasm within 60 min incubation. Cells in the white boxed area are shown at a higher magnification in the right panels. Bars, 10 μm.

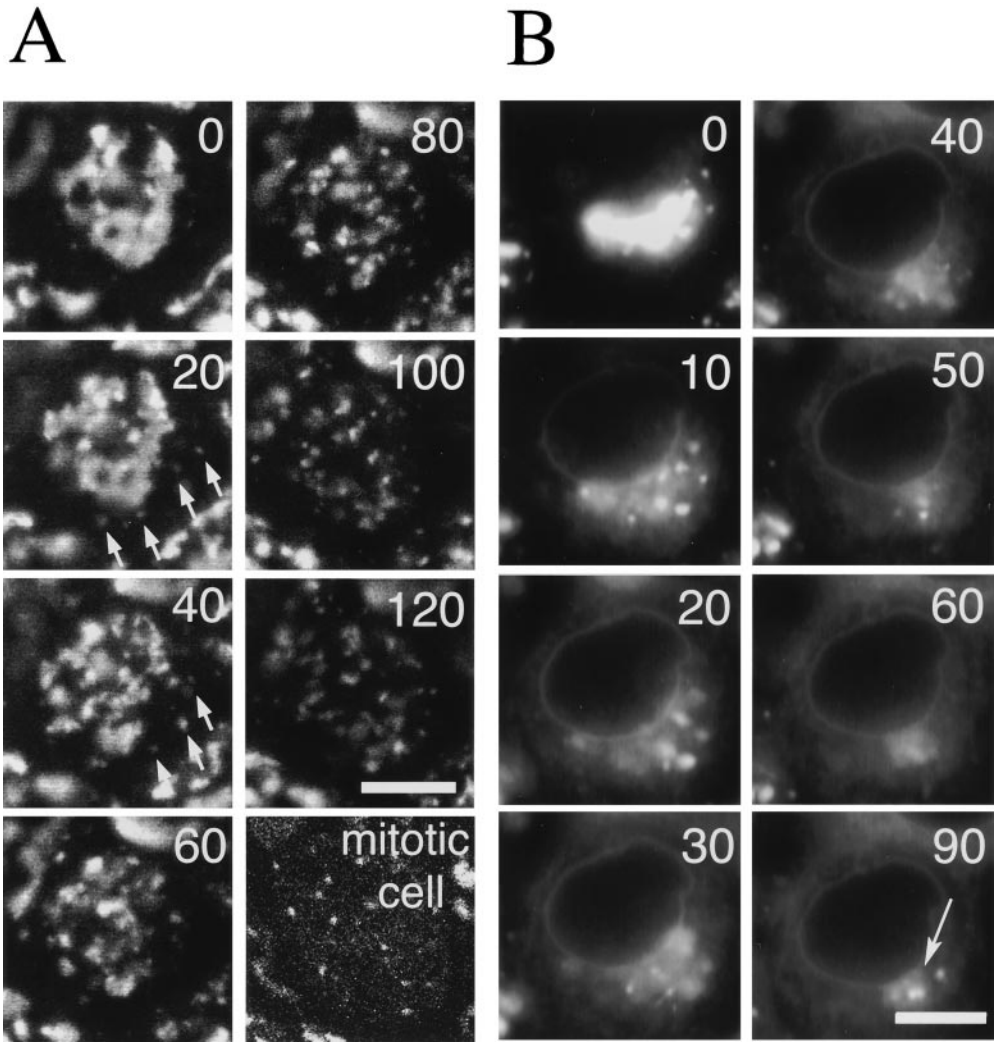

Figure 3. Morphological changes during the Golgi disassembly in a single semi-intact cell. (A) MDCK-GT cells were incubated with *Xenopus* egg extracts and ATP at 28°C for the indicated period. Images were collected every 10 min using a confocal microscope. Although the disassembly process progressed halfway probably due to damage from the repeated laser scans, punctate structures budding from the Golgi structures were frequently observed (arrows). As a control, mitotic Golgi membranes labeled with GFP in intact MDCK-GT cells are shown in the last panel. (B) A similar process was observed in semi-confluent cultured cells using a conventional microscope. Perinuclear Golgi cisternae were disorganized into punctate structures by the 10 min incubation. The punctate structures began to fragment further at ~30 min and had entirely dispersed within 60 min. Fluorescent membranous remnants were observed even at the final stage of mitotic Golgi membranes (arrow). Bars, 10 μm.

peared and highly dispersed profiles of Golgi membranes appeared throughout the cytoplasm. The Golgi punctate structures seem to be intermediates in the disassembly process, and the highly dispersed profiles might be attributable to the further processing state of Golgi disassembly.

The Golgi disassembly process was followed in a single cell. A semi-intact MDCK-GT cell in the presence of *Xenopus* egg extracts and ATP was observed on the stage of a confocal microscope (incubation at 28°C) and imaged at 5-min intervals (Fig. 3 A). At the 0 time point, the Golgi apparatus localized in a perinuclear region as a typical ribbon-shape. Within 40 min, small vesicles began to bud from the large stacks of Golgi. After 60 min incubation, the main stacks of Golgi apparatus were broken down to the smaller punctate structures. Unfortunately, we could not follow the process any further, because of damage to the samples by repeated laser scans. During the 100-min time-lapse observation, we did not see the diffusive ER network pattern of GT-GFP. This suggests that the punctate structures are not produced via the ER but from the large stacks of Golgi directly (see Discussion).

We were able to follow the process in a single, semi-confluent cultured MDCK-GT cell using a conventional fluorescence microscope (Fig. 3 B). Within 10 min incubation, the Golgi punctate structures appeared and they were likely to localize in a perinuclear region. The outlines of these large punctate structures began to blur after 30 min incubation. The rim of nucleus concurrently became brighter. Such staining of the nuclear envelopes indicates that the diffusive GT-GFP localizes to the ER (see next section). On further incubation (<60 min), the punctate structures became fully dispersed throughout the cytoplasm. Interestingly, several fluorescent vesicles remained intact in the region where the Golgi apparatus was first located. Such membranous remnants and time-dependent morphological changes were previously observed in living HeLa cells during mitotic phase (Shima et al., 1998).

Morphological Dissection of the Golgi Disassembly in Semi-intact Cells

Based on microscopic observation of the Golgi morphology, we divided the disassembly process into three stages; stage I (intact), II (punctate), and III (dispersed). The confocal sectioning images at each stage are shown in Fig. 4, A–C. At stage I (intact), tubular and stacking structures of a typical intact Golgi apparatus were observed in the perinuclear region through the apical to middle part of the

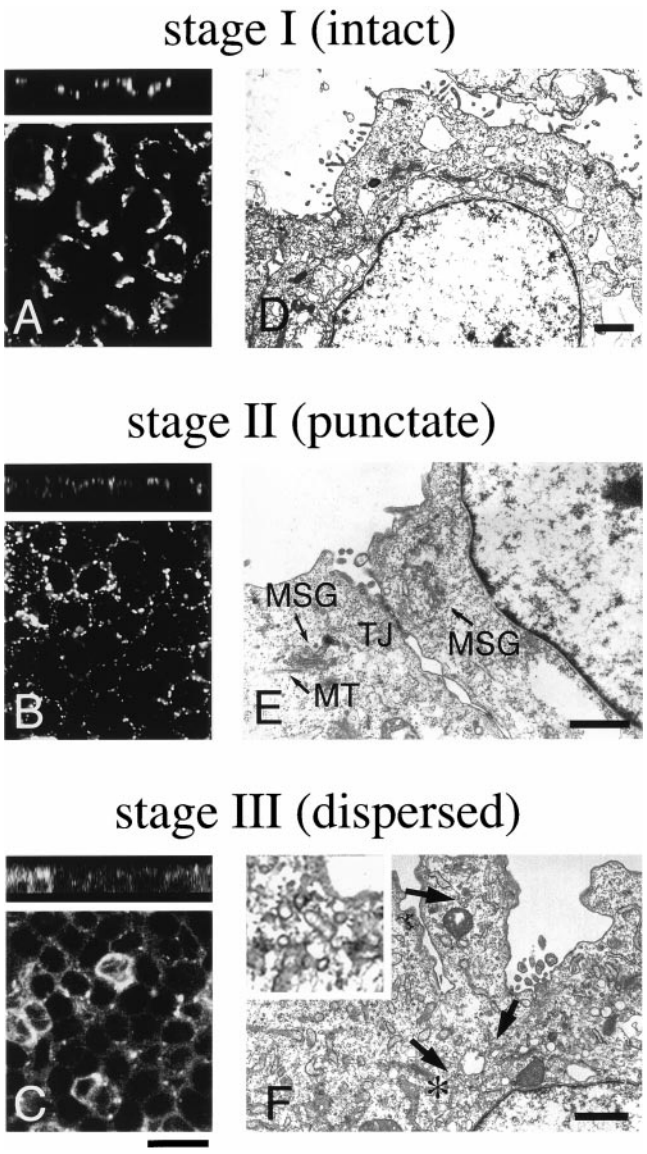

Figure 4. Morphological dissection of the Golgi disassembly process in semi-intact cells. For the morphometric analysis, we divided the disassembly process into three stages based on the Golgi morphology: stage I (intact); intact perinuclear Golgi cisternae (A), stage II (punctate); punctate structures on the apical side of the nucleus (B), stage III (dispersed); highly dispersed Golgi membranes throughout the cytoplasm (C). Cells at each stage were observed by confocal microscope. The lower panel shows xy images in an apical region of the cells and the upper panel shows xz sectioning images. Electron microscopic images of cells at each stage are shown in D (stage I), E (stage II), and F (stage III). (D) Control without egg extracts (stage I). A large stack of cisternae of the Golgi apparatus is seen at the apical side of the cell. (E) 80 min after incubation with egg extracts containing cdc2 kinase inhibitor (stage II). Mini-stacked Golgis (MSG) are seen at the apical side of the cells, where tight junction (TJ) is observed. Mini-stacked Golgi associates with microtubules (MT). (F) 80 min after incubation with egg extracts (stage III). No stacked structure of the Golgi apparatus is observed, and only tubulo-vesicular structures (arrows), which probably derived from the Golgi, are seen. Inset represents the tubulo-vesicular structures (asterisk) at a higher magnification. Bars: (A–C) 20 μm; (D–F) 1 μm.

cells (Fig. 4 A and stage I in Fig. 6). At stage II (punctate), Golgi punctate structures were observed on mainly the apical side of the nucleus (Fig. 4 B and stage II in Fig. 6). These punctate structures were seldom seen in the basolateral cytoplasm. At stage III (dispersed), diffusive staining pattern was observed throughout the cytoplasm (Fig. 4 C and stage III in Fig. 6). The cells, which have both punctate and dispersed profiles of Golgi morphology, are also defined as stage II.

Electron microscopic observations showed that the stacks of cisternae were on the apical side of the nucleus in stage I (intact) cells. After permeabilization, tight junctions were clearly shown (TJ in Fig. 4 E), from which we can identify the apical side of the cell. In stage II (punctate), the small stacked cisternae were found in an apical region. The mini-stack Golgi were ~800 nm in diameter, associating with microtubules (MSG; mini-stack Golgi in Fig. 4 E). These mini-stack Golgi were not found in the basolateral region. Few unstacked Golgi fragments were observed at stage II. To observe the ultrastructural features in stage II easily, we treated the semi-intact cells with *Xenopus* egg extract containing a specific inhibitor for cdc2 kinase, butyrolactone I (BL), for 80 min. Because, in the presence of BL containing egg extract, ~80% of cells showed the Golgi profiles in stage II (described in detail later). Fig. 4 F shows the tubulo-vesicular Golgi fragments at stage III (dispersed). The Golgi tubulo-vesicular structures, which were probably derived from the Golgi, located throughout the cytoplasms. Thus, the Golgi morphology and its intracellular location were changed at each of the three stages.

Interestingly, at light microscopy level, the staining of the nuclear envelopes was frequently observed in the cells at stage III (>80% of cells). This is indicative of the ER staining and means that the Golgi component (in our case, GT-GFP) relocated to the ER during the Golgi disassembly. To test this, at first we treated the intact cells with cycloheximide (10 μg/ml for 3 h) to rule out the signal due to the newly synthesized protein that gets stuck in the ER because of the protein-transport block in our experimental conditions. Then we performed the Golgi disassembly assay and observed the Golgi morphology at each stage by a confocal microscope. As we expected, in the cells at stage III, extensive staining pattern of the nuclear envelope and ER-like networks in the apical or basolateral regions were frequently observed (Fig. 5 A, stage III), but such pattern was rarely seen in the cells at stage II (<20% of cells; Fig. 5 A, stage II). Next, we examined the colocalization of GT-GFP with the ER-specific marker protein, PDI, by indirect immunofluorescence method (Fig. 5 B). We detected the extensive overlap in the distribution of GT-GFP and PDI in the nuclear envelopes and the partial overlap in the ER-like networks. There was a subtle difference in staining pattern, which may reflect differences in localization of two proteins either in the ER or in the vesicles at stage III. The results suggest that the GT-GFP substantially relocated to the ER during the Golgi disassembly (most likely from stage II to stage III). However, the diffusive staining pattern throughout the cytoplasm and the small vesicular structures were still observed in the cells at stage III. Unfortunately, the conventional electron microscopic observation (TEM) we used here is not suitable for confirming the relocation of the Golgi components to the ER at stage III.

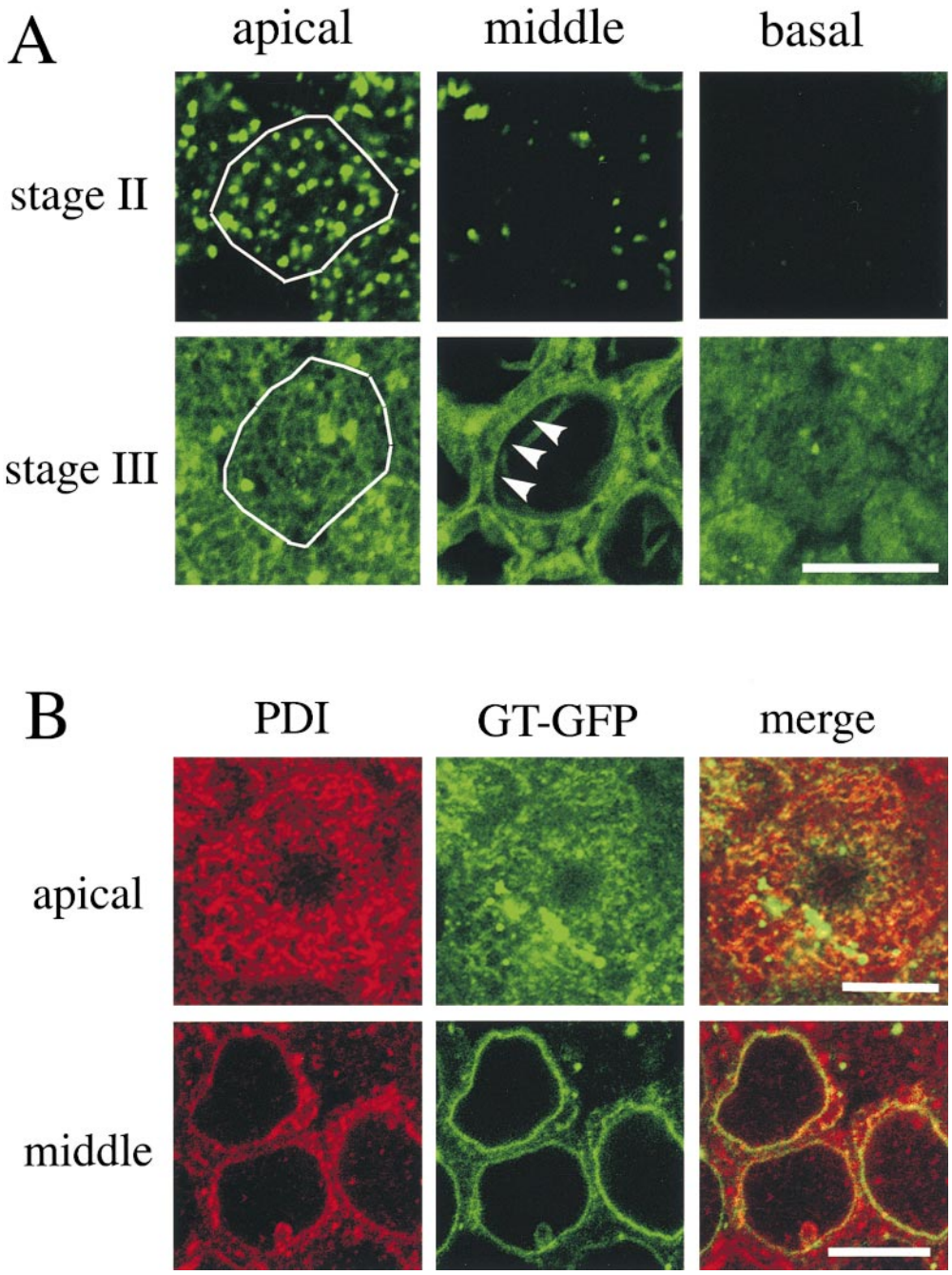

Figure 5. Relocation of the GT-GFP to the ER during the Golgi disassembly. (A) Intact MDCK-GT cells were treated with cycloheximide (10 μg/ml for 3 h) and then subjected to the permeabilization. Semi-intact MDCK-GT cells were incubated with either *Xenopus* egg extracts and ATP with cdc2 inhibitor (stage II), or *Xenopus* egg extracts and ATP (stage III) at 33°C for 80 min. The typical distributions of GT-GFP in the apical, middle and basal regions in the cells at each stage are visualized with a confocal microscope. White lines indicate the periphery of single cells. Extensive staining of the nuclear envelopes (middle region) and the ER-like networks (apical and basal regions) are observed most likely at stage III. The stained nuclear envelope is indicated by arrowheads. (B) The GT-GFP and the ER specific marker, PDI, at stage III were double stained and visualized with a confocal microscope. Extensive overlap in the distribution of GT-GFP and PDI in the nuclear envelopes (middle) and partial overlap in the ER-like networks (middle and apical regions of the cells) were detected. Bars, 10 μm.

We have investigated the interaction between the Golgi membranes and microtubules at each stage by an immunofluorescence method using anti–α-tubulin antibody. At stage I, the Golgi tubular structures and stacks were found to associate with microtubules on the apical side of the nucleus (Fig. 6 A, stage I). The Golgi punctate structures at stage II also localized with the apical network of microtubules. They were not associated with the basolateral microtubule array (Fig. 6 B, stage II). The Golgi membranes at stage III were fully dispersed throughout the cytoplasm (Fig. 6, stage III). Microtubule integrity in semi-intact cells was intact morphologically after >90 min incubation with *Xenopus* egg extracts and ATP at 33°C.

Kinetic Analysis of the Golgi Disassembly in Semi-intact Cells

After incubation for various times, cells were fixed and the numbers of cells at stage I, II, and III were counted (Fig. 7). The percentage of stage I (intact) cells decreased to ~20% by the 30-min incubation, and stage III (dispersed) cells increased to ~40%. Stage II (punctate) cells increased and reached maximum (40%) at 30 min then decreased to ~20% as the incubation proceeded. The time-dependent increase followed by the decrease in the percentage of stage II (punctate) cells suggests that the punctate structures are the intermediates in the process of Golgi disassembly. Since the Golgi disassembly process reached a

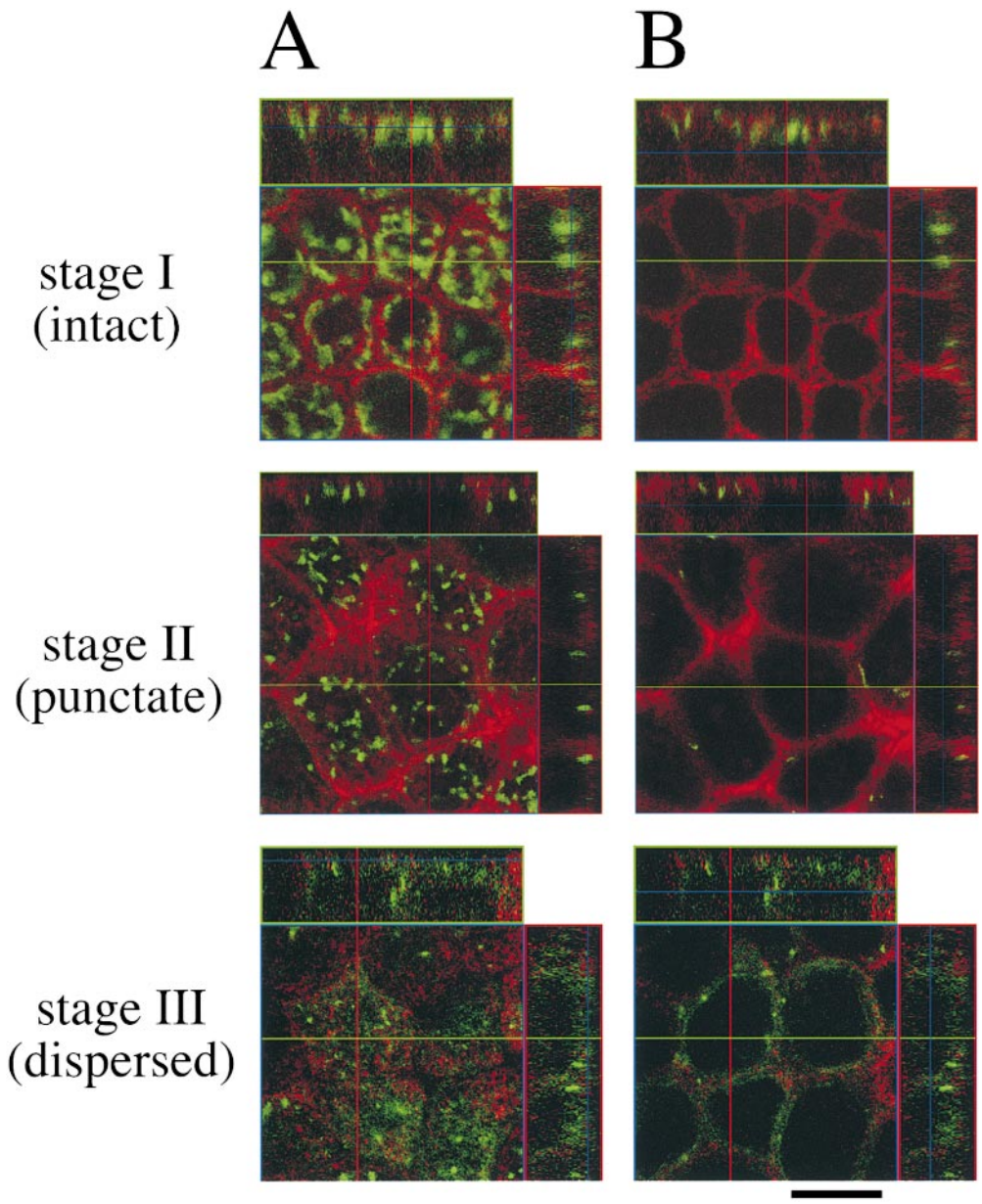

Figure 6. Intracellular configurations of the Golgi membranes and microtubules at each stage. Semi-intact MDCK-GT cells were incubated with either ATP in TB (stage I), *Xenopus* egg extracts and ATP with cdc2 inhibitor (stage II), or *Xenopus* egg extracts and ATP (stage III) at 33°C for 80 min. The Golgi membranes and microtubules at each stage were double stained and visualized with a confocal microscope. The apical region (A, h = 9.2 μm from the base), and middle region (B, h = 5.4 μm) of the cells at each stage are shown. The Golgi membranes are indicated by green, and the microtubules by red. At stage II, punctate Golgi membranes associated with apical microtubule networks. At stage III, the Golgi membrane was dispersed throughout the cytoplasm. Bar, 10 μm.

steady-state within ~80–90 min incubation, we fixed the experimental conditions (incubation at 33°C for 80 min) to evaluate the biochemical requirements for the following experiments.

Cdc2 and MEK Are Involved in the Golgi Disassembly

We tested the effect of various kinase inhibitors on the Golgi disassembly in semi-intact systems (Fig. 8). Staurosporine (SS), a broad-range kinase inhibitor, inhibited the Golgi disassembly. In the presence of SS, the percentage of the stage III cells decreased to ~25% from ~70% in the absence of the inhibitor. Butyrolacotone I (BL), a specific inhibitor of cdc2, and PD98059 (PD), a specific inhibitor of MEK, showed dramatic effects. In the presence of BL, ~80% of cells showed the Golgi punctate profiles (stage II). Continued incubation (~120 min) of the samples did not change the percentages of each stage further. In the presence of PD, ~45% of the cells remained in the stage I (intact). A similar result was obtained by using another MEK inhibitor, U0126 (data not shown). In the presence of both BL and PD, the Golgi disassembly was completely inhibited (Fig. 8, BL+PD). SB203580 (SB), a specific inhibitor of p38 subfamily member of MAP kinase, had no effect on the Golgi disassembly. These results suggest that both cdc2 and MEK are involved in the Golgi disassembly, and MEK is mainly involved in the first step (from stage I to II), and cdc2 in the second step (from stage II to III).

We then performed immunodepletion experiments using mouse anti-cdc2 monoclonal antibodies and rabbit anti-MEK polyclonal antibodies. Specific depletion of cdc2 or MEK from *Xenopus* egg extracts was confirmed by Western blotting (Fig. 9 A). Either cdc2- or MEK-depleted extracts were added to the salt-washed, semi-intact cells. In the presence of cdc2-depleted extracts, the punctate Golgi structures were found in 90% of cells. MEK-

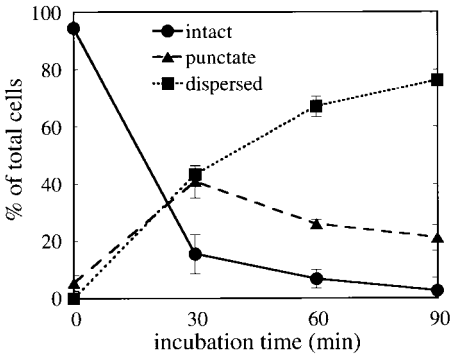

Figure 7. Kinetics of Golgi disassembly in semi-intact cells. Semi-intact cells were incubated with *Xenopus* egg extracts and ATP at 33°C for the indicated period. After incubation, the cells were fixed and morphometric analysis was performed. Time-dependent changes in the percentages of cells at each stage are shown. The protein concentration of the extract used was 5.0 mg/ml. 300 cells were counted in three randomly selected fields, and standard deviations are shown as vertical bars.

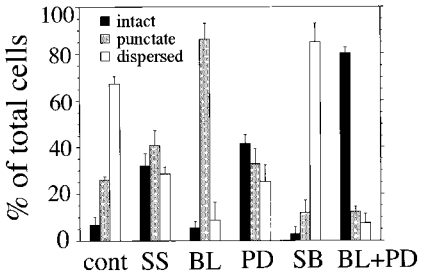

Figure 8. Effect of protein kinase inhibitors on the Golgi disassembly. Semi-intact MDCK-GT cells were incubated with *Xenopus* egg extracts and ATP containing either no inhibitor (control), staurosporine (SS), butyrolactone l (BL), PD98059 (PD), SB203580 (SB), or BL+PD, respectively, at 33°C for 80 min. Then cells were fixed and morphometric analysis was performed as described in the legend of Fig. 7.

depleted extract also inhibited the Golgi disassembly at stage I (intact) in ~60% of cells (Fig. 9 B). These results were consistent with the effects of kinase inhibitors and supported our model that cdc2 is responsible for the process from stage II to III, and MEK from stage I to II.

Golgi Disassembly Induced by Cdc2- or MEK-activated Interphase Extracts

Both cdc2 and MEK are usually inactivated in *Xenopus* interphase extract. Indeed, in our system, *Xenopus* interphase extracts did not cause the Golgi disassembly (Fig. 1 C). If our idea is correct, when cdc2 or MEK is activated the interphase extracts should cause the disassembly. To test this, we incubated the interphase extracts (I) with cyclin A (C), STE11 (S), or both (SC) for 60 min to activate cdc2, MEK, or both, respectively, and prepared three types of the interphase extracts, IC, IS, or ISC, respectively. Cyclin A is a cofactor of cdc2. The complex formation between cdc2 and cyclin A is able to activate cdc2 kinase activity (Roy et al., 1991). STE11 is the yeast MAP kinase kinase and is known to phosphorylate and activate MEK (Gotoh et al., 1995). Cdc2 or MEK activation in interphase extracts was confirmed by in vitro kinase assays (Fig. 10 A). The STE11 treatment increased specifically the MEK activity of the interphase extracts 1.3-fold (Fig. 10 A, I+STE), and the cyclin A treatment increased the cdc2 activity ~8-fold (Fig. 10 A, I+cycA). Under the condition used, cyclin A did induce the activation of MEK. We added the MEK inhibitor, PD, to the IC extracts to inhibit the residual MEK activity for subsequent experiments.

As shown in Fig. 10 B, the Golgi apparatus remained intact after incubation with normal interphase extracts. In contrast, MEK-activated interphase extracts (IS) induced extensive disassembly of the Golgi membranes in >60% of cells. Cdc2-activated interphase extracts (IC) less potently caused the Golgi disassembly than the IS extract; the percentages of stage I (intact) and stage II (punctate) cells were both ~40%. The MEK and cdc2-activated interphase extracts (ISC) caused Golgi disassembly fully (Fig. 10 B, ISC). Incubation with only cyclin A or STE11 in the absence of extracts did not cause Golgi disassembly (Fig. 10 B, STE, cycA).

We have tested the sequential effect of cdc2 and MEK on the Golgi disassembly. After incubation with IS or IC, the cells were further incubated with IC or IS (Fig. 10 B, IS-IC or IC-IS). The IS-IC incubation caused the Golgi disassembly fully, like the ISC. In contrast, the Golgi disassembly was partial in the IC-IS incubation. The degree of Golgi disassembly was almost the same as that in cells incubated only with IC.

Taken together, our results indicate that the cdc2- and MEK-activated *Xenopus* interphase extracts can induce the Golgi disassembly like mitotic phase extracts, and suggest that cdc2 and MEK are sequentially involved in the Golgi disassembly: MEK most likely in the first step (from stage I to II) and cdc2 in the second step (from stage II to III).

Discussion

Mitotic Golgi disassembly is a dynamic and highly regulated process, and required for an equal partitioning of Golgi membranes into two daughter cells. From recent analyses of the disassembly steps in living cells by using GFP-visualization techniques, two mechanisms have been proposed: the Golgi fragmentation model by Warren (1993) and the Golgi absorption model by Zaal et al. (1999). Moreover, the in vitro systems have been developed to study the process, and biochemical requirements for protein kinases have been analyzed (Lowe et al., 1998; Acharya et al., 1998).

One of the aims of this study is to establish a reconstitution system for the mitotic Golgi disassembly in polarized cells and dissect the process morphologically and biochemically. First, we used a bacterial pore forming toxin, SLO, to prepare the semi-intact MDCK-GT cells. The method was established and refined by Simons' group to study the polarized vesicular traffic in MDCK cells by exchanging the cytoplasmic proteins or adding antibodies (Pimplikar et al., 1994; Ikonen et al., 1995). Even after permeabilization, MDCK cells forming an epithelial sheet on polycarbonate membranes are highly polarized and main-

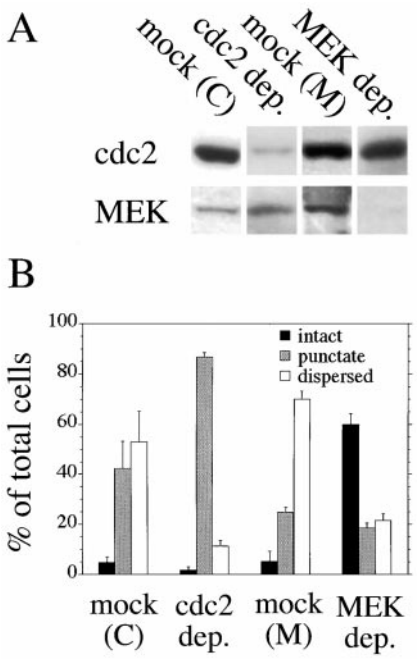

Figure 9. Inhibition of the Golgi disassembly by cdc2- or MEK-depleted *Xenopus* egg extracts. (A) Immunoblotting of mock for MEK-depleted, MEK-depleted, mock for cdc2-depleted, and cdc2-depleted *Xenopus* egg extracts with anti-cdc2 (top) and anti-MEK (bottom) antibodies. (B) Mock, cdc2- or MEK-depleted *Xenopus* egg extracts were applied to semi-intact cells and incubated at 33°C for 80 min. The cells were fixed and morphometric analysis was performed as described in the legend of Fig. 7. Cdc2-depleted extracts arrested the disassembly process at stage II (punctate), and MEK-depleted extracts did so at stage I (intact).

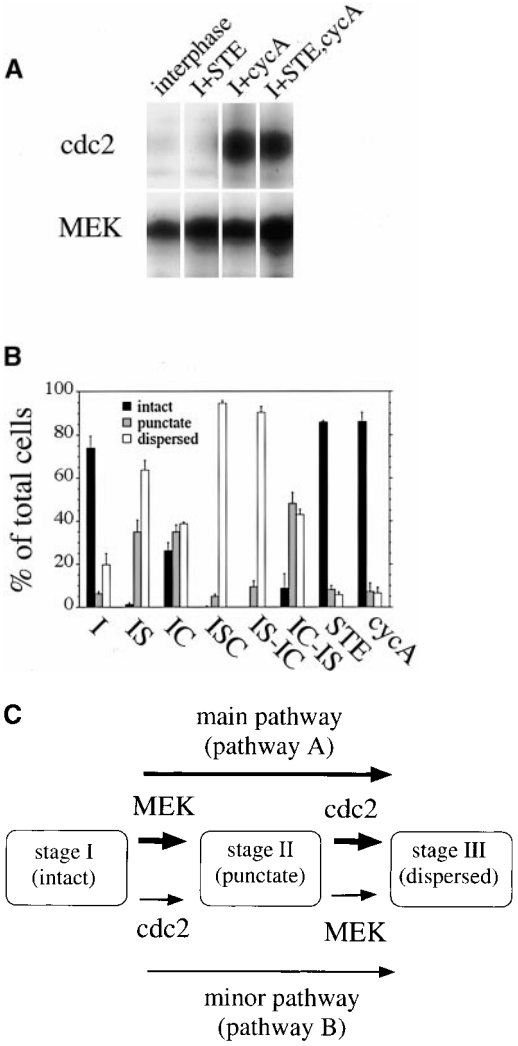

Figure 10. Induction of the Golgi disassembly by cdc2- or MEK-activated *Xenopus* interphase extracts. Three types of *Xenopus* interphase extracts, cdc2-activated extract (IC), MEK-activated extract (IS) and cdc2/MEK-activated extract (ISC), were prepared as described in Materials and Methods. (A) Cdc2 and MEK activation in the interphase extracts was confirmed by in vitro kinase assay. (B) Semi-intact cells were incubated with each extract (protein concentration at 5.0 mg/ml) at 33°C for 80 min, fixed and then cells were analyzed by morphometric analysis as described in the legend of Fig. 7. For IS-IC or IC-IS, semi-intact cells were incubated with IS (or IC) at 33°C for 40 min. After washing, cells were further incubated with IC (or IS) for 40 min. Then they were fixed and subjected to morphometric analysis. Incubation of the semi-intact cells with only STE11 (STE) or cyclin A (cycA) did not result in the Golgi disassembly. (C) A model for the Golgi disassembly induced by *Xenopus* egg extracts. The Golgi disassembly pathway in semi-intact MDCK-GT cells was dissected into two elementary processes. Both cdc2 and MEK might be involved in two processes, but the contribution of each kinase might depend on the cell type, the intracellular physiological conditions or the cell architecture such as microtubule stability. In our reconstitution system, a sequential requirement of MEK and cdc2 in that order (pathway A) seems to be the prominent pathway, and pathway B a minor one.

tain their intracellular architecture and topology of cytoskeletons and organelles. The dynamics of Golgi membranes labeled with GFP proteins could be followed for >1 h under a confocal microscope. Second, we used *Xenopus* egg extracts, in which the cell cycle is arrested at metaphase, for the mitotic phase extracts. The *Xenopus* egg extracts give us several advantages; the large-scale preparation is easy, and the extract has a high protein concentration and is highly synchronized in mitotic phase. However, it should be noted that there are several differences between *Xenopus* egg extracts and mammalian mitotic phase cytosol. For example, both cdc2 and MEK are extensively active in *Xenopus* egg extracts while only cdc2 is highly activated in mammalian mitotic cytosol. Despite these differences, incubation with *Xenopus* egg extracts, but not with *Xenopus* interphase extracts, caused extensive dispersion of Golgi membranes (Fig. 1). There would be common molecules in *Xenopus* egg extracts and mammalian mitotic phase cytosol, which induce the Golgi disassembly.

Morphological Dissection of the Mitotic Golgi Disassembly

Monitoring the time-dependent changes of Golgi morphology both in numerous fixed cells and in a single, semi-intact cell during disassembly, we have found that the Golgi cisternae first break into large punctate structures,

which subsequently fragment further and disperse throughout the cytoplasm (Figs. 2 and 3, A and B). The two-step disassembly of Golgi apparatus was noted previously in mitotic living cells visualized by GFP-tagged proteins (Shima et al., 1998; Zaal et al., 1999) and by electron microscopic observations (Misteli and Warren, 1995). Our study is the first to demonstrate clearly the two steps of the mitotic Golgi disassembly process in semi-intact cells using GFP-tagged Golgi resident proteins.

We classified the Golgi morphology into three. In stage I (intact), the Golgi cisternae surround the nucleus as tubulo-cisternal structures. In stage II (punctate), the fragmented Golgi membranes segregated from the vine of the Golgi apparatus. In stage III (dispersed), the Golgi membranes completely dispersed throughout the cytoplasm. Our results suggest that the punctate structure (stage II) is an intermediate of the mitotic Golgi disassembly process.

Electron microscopic observations revealed that large stacks of cisternae are present in the apical region of semi-intact MDCK-GT cells at stage I. At stage II, many smaller Golgi-like stacks interacting with apical microtubules are present (Fig. 4 E). It is noted that each stack comprises several cisternae like the intact Golgi but the average length is shorter ($\sim$0.8 μm) than that of intact Golgi ($\sim$6 μm). At stage III, neither cisternae nor smaller Golgi-like stacks are seen. Rather, the Golgi membrane disperses throughout the cytoplasm (Fig. 4 F).

Our time-lapse observation during the early step of the disassembly detected neither the diffusive ER network nor the nuclear envelope staining by GT-GFP (Fig. 3 A). However, during the late step, light microscopic observations in Figs. 3 B and 5 revealed that the nuclear envelope and the ER-like networks were substantially stained in the cells most likely at stage III. These results suggest that the relocation of Golgi component (GT-GFP) to the ER did occur during the Golgi disassembly. In addition, more extensive staining of the nuclear envelopes at stage III rather than at stage II indicates that relocation to the ER might occur most likely in the late process of the disassembly.

Thus, we conclude that the Golgi first becomes converted into the punctate structures and then undergoes further processing. Recently, using quantitative imaging and photobleaching techniques, Zaal et al. (1999) demonstrated that the Golgi components are absorbed into the ER during mitosis and subsequently reemerge to form a perinuclear Golgi complex. At this stage, it is difficult for us to address whether the Golgi membranes are ultimately converted into the vesicles or fuse with the ER. Although we have still observed the tubulo-vesicular structures in the cells at stage III by the electron microscopic observation (TEM experiment in Fig. 4 F), the light microscopic observation described above clearly indicates that the Golgi components substantially relocate to the ER connecting to the nuclear envelopes. Thus, our results could be consistent with the findings of Zaal et al. (1999) concerning the Golgi disassembly process in mitotic living cells. However, this problem remains to be solved and needs more extensive experiments, especially by immunoelectron microscopy.

In polarized MDCK cells, microtubules form long cortical filaments parallel to the lateral membrane, a meshwork of randomly oriented short filaments beneath the apical membrane and short filaments at the base of the cell (Meads and Schroer, 1995; Grindstaff et al., 1998). Both intact and punctate Golgi membranes in our reconstitution system are located in the subapical membrane cytoplasm, interacting with the apical meshwork of microtubules. Therefore, we suppose that the first step of disassembly (from stage I to II) is regulated by microtubule integrity.

Biochemical Dissection of the Mitotic Golgi Disassembly

Previously, two reports revealed the requirement of protein kinases, cdc2 or MEK, for the Golgi disassembly process (Acharya et al., 1998; Lowe et al., 1998). But their results were not consistent with each other. In our studies, inactivation or depletion of cdc2 in *Xenopus* egg extracts arrests the Golgi disassembly process at stage II (punctate). In contrast, inactivation or depletion of MEK inhibits the initiation of Golgi disassembly (Figs. 8 and 9). These and other results indicate that both kinases are required for the Golgi disassembly and MEK is mainly involved in the first step (from stage I to II) and cdc2 in the second (from stage II to III). We now hypothesize that the initial fragmentation induced by MEK may be for the subsequent thorough dispersion by cdc2. Each kinase, however, does not seem to correspond to each step independently. Both kinases might have overlapping functions. In fact, the specific activation of either cdc2 or MEK in interphase extracts is able to cause the Golgi disassembly to some extent. Moreover, a combination of a cdc2 inhibitor (BL) and a MEK inhibitor (PD) completely inhibits the *Xenopus* egg extracts–induced disassembly, but PD alone does not inhibit the process completely.

Our current hypothesis is schematically shown in Fig. 10 C, which assumes two pathways. In the main pathway (A), MEK is involved in the first step and cdc2 in the second one, and in the minor pathway (B) cdc2 in the first and MEK in the second.

Several lines of evidence support the above model and the predominant pathway A in Fig. 10 C. Most recently, MEK has been reported to play some roles in the induction of the early mitotic events and/or the determination of the timing for entry to mitosis. Wright et al. (1999) reported that ectopic expression of dominant-negative MEK delayed progression of cells from G2 to mitosis in NIH 3T3 cells. They also showed that careful treatment of PD caused the inhibition of mitosis entry in intact cells, although Warren and colleagues had reported the inefficiency of PD treatment on the entry into mitosis and the Golgi fragmentation (Lowe et al., 1998). In addition, Bitangcol et al. (1998) demonstrated that the inappropriate activation of MAPK during interphase prevented entry into mitosis in cycling *Xenopus* egg extracts. These results indicate the involvement of MEK in the early mitotic events.

However, in living cells and in other cell systems, it is not yet clear what the relative contribution of each of these two pathways (pathways A or B in Fig. 10 C) is. For example, it should be noted that when the microtubules in semi-intact cells were made unstable by lack of taxol treatment, the inhibitory effect of PD on the first process was

reduced. In contrast, the effect of BL was unchanged (Kano, F., and M. Murata, unpublished data). MEK action in the first step may be dependent on microtubule integrity, whereas cdc2 action may not. In addition, morphological observations revealed that the punctate Golgi (stage II) membranes interact with microtubules. The contribution of each pathway may be determined by other intracellular factors such as microtubule instability, which are not completely reconstituted in our assay system.

We cannot rule out the possibility that other kinases, which might be retained in semi-intact cells or tightly associated with Golgi membranes, are involved in the Golgi disassembly. For example, ERK-type MAP kinase was found to bind tightly to the Golgi membranes in digitonin-permeabilized NRK cells (Acharya et al., 1998).

Our reconstitution systems, based on semi-intact cells coupled with GFP visualization techniques, will be of use in manipulating intracellular conditions for observing the morphological changes of GFP-tagged organelles under a fluorescence microscope. The system allows us to dissect complex reaction processes in cells morphologically and to screen and investigate the biochemical requirements and kinetics for each process, for example the disassembly and reassembly of Golgi during mitosis.

We would like to thank Dr. M. Furuse at Kyoto University for providing the mouse liver cDNA library and for helpful discussions. We also thank Dr. R. Masaki at Kansai Medical University for generously providing the rabbit antiserum against rat PDI.

This work was supported by a Grant-in-Aid for Scientific Research on Priority Areas (B) from the Ministry of Education, Science, Sports and Culture of Japan (M. Murata) and by a JSPS Research Fellowship for Young Scientists (F. Kano).

Submitted: 29 September 1999
Revised: 10 March 2000
Accepted: 14 March 2000

References

Acharya, U., A. Mallabiabarrena, J.K. Acharya, and V. Malhotra. 1998. Signaling via mitogen-activated protein kinase kinase (MEK1) is required for Golgi fragmentation during mitosis. *Cell.* 92:183–192.

Akagi, S., A. Yamamoto, T. Yoshimori, R. Masaki, R. Ogawa, and Y. Tashiro. 1988. Distribution of protein disulfide isomerase in rat hepatocytes. *J. Histochem. Cytochem.* 36:1533–1542.

Barak, L.S., R.R. Yocum, E.A. Nothnagel, and W.W. Webb. 1980. Fluorescence staining of the actin cytoskeleton in living cells with 7-nitrobenz-2-oxa-1,3-diazole-phallacidin. *Proc. Natl. Acad. Sci. USA.* 77:980–984.

Bitangcol, J.C., A.S. Chau, E. Stadnick, M.J. Lohka, B. Dicken, and E.K. Shibuya. 1998. Activation of the p42 mitogen-activated protein kinase pathway inhibits Cdc2 activation and entry into M-phase in cycling *Xenopus* egg extracts. *Mol. Biol. Cell.* 9:451–467.

Chau, A.S., and E.K. Shibuya. 1998. Mos-induced p42 mitogen-activated protein kinase activation stabilizes M-phase in *Xenopus* egg extracts after cyclin destruction. *Biol. Cell.* 90:565–572.

Cole, N.B., C.L. Smith, N. Sciaky, M. Terasaki, M. Edidin, and J. Lippincott-Schwartz. 1996. Diffusional mobility of Golgi proteins in membranes of living cells. *Science.* 273:797–801.

Ellenberg, J., E.D. Siggia, J.E. Moreira, C.L. Smith, J.F. Presley, H.J. Worman, and J. Lippincott-Schwartz. 1997. Nuclear membrane dynamics and reassembly in living cells: targeting of an inner nuclear membrane protein in interphase and mitosis. *J. Cell Biol.* 138:1193–1206.

Gotoh, Y., N. Masuyama, K. Dell, K. Shirakabe, and E. Nishida. 1995. Initiation of *Xenopus* oocyte maturation by activation of the mitogen-activated protein kinase cascade. *J. Biol. Chem.* 270:25898–25904.

Grindstaff, K.K., R.L. Bacallao, and W.J. Nelson. 1998. Apiconuclear organization of microtubules does not specify protein delivery from the trans-Golgi network to different membrane domains in polarized epithelial cells. *Mol. Biol. Cell.* 9:685–699.

Guadagno, T.M., and J.E. Ferrell, Jr. 1998. Requirement for MAPK activation for normal mitotic progression in *Xenopus* egg extracts. S*cience.* 282:1312–1315.

Hughson, E.J., and R.P. Hirt. 1996. Assessment of cell polarity. *In* Epithelial Cell Culture. A.J. Shaw, editor. Oxford University Press, Oxford. 37–66.

Ikonen, E., M. Tagaya, O. Ullrich, C. Montecucco, and K. Simons. 1995. Different requirements for NSF, SNAP, and Rab proteins in apical and basolateral transport in MDCK cells. *Cell.* 81:571–580.

Kosako, H., Y. Gotoh, and E. Nishida. 1994. Requirement for the MAP kinase kinase/MAP kinase cascade in *Xenopus* oocyte maturation. *EMBO (Eur. Mol. Biol. Organ.) J.* 13:2131–2138.

Lowe, M., C. Rabouille, N. Nakamura, R. Watson, M. Jackman, E. Jamsa, D. Rahman, D.J. Pappin, and G. Warren. 1998. Cdc2 kinase directly phosphorylates the cis-Golgi matrix protein GM130 and is required for Golgi fragmentation in mitosis. *Cell.* 94:783–793.

Mackay, D., R. Kieckbusch, J. Adamczewski, and G. Warren. 1993. Cyclin A-mediated inhibition of intra-Golgi transport requires p34 cdc2. *FEBS Lett.* 336:549–554.

Meads, T., and T.A. Schroer. 1995. Polarity and nucleation of microtubules in polarized epithelial cells. *Cell Motil. Cytoskeleton.* 32:273–288.

Misteli, T., and G. Warren. 1994. COP-coated vesicles are involved in the mitotic fragmentation of Golgi stacks in a cell-free system. *J. Cell Biol.* 125: 269–282.

Misteli, T., and G. Warren. 1995. A role for tubular networks and a COP I-independent pathway in the mitotic fragmentation of Golgi stacks in a cell-free system. *J. Cell Biol.* 130:1027–1039.

Murray, A.W. 1991. Cell cycle extracts. *Methods Cell Biol.* 36:581–605.

Nakamura, N., C. Rabouille, R. Watson, T. Nilsson, N. Hui, P. Slusarewicz, T.E. Kreis, and G. Warren. 1995. Characterization of a cis-Golgi matrix protein, GM130. *J. Cell Biol.* 131:1715–1726.

Nigg, E.A. 1995. Cyclin-dependent protein kinases: key regulators of the eukaryotic cell cycle. *Bioessays.* 17:471–480.

Nishida, E., and Y. Gotoh. 1993. The MAP kinase cascade is essential for diverse signal transduction pathways. *Trends Biochem. Sci.* 18:128–131.

Pimplikar, S.W., E. Ikonen, and K. Simons. 1994. Basolateral protein transport in streptolysin *O*-permeabilized MDCK cells. *J. Cell Biol.* 125:1025–1035.

Roy, L.M., K.I. Swenson, D.H. Walker, B.G. Gabrielli, R.S. Li, H. Piwnica-Worms, and J.L. Maller. 1991. Activation of p34cdc2 kinase by cyclin A. *J. Cell Biol.* 113:507–514.

Schnaar, R.L., P.H. Weigel, M.S. Kuhlenschmidt, Y.C. Lee, and S. Roseman. 1978. Adhesion of chicken hepatocytes to polyacrylamide gels derivatized with N-acetylglucosamine. *J. Biol. Chem.* 253:7940–7951.

Shima, D.T., K. Haldar, R. Pepperkok, R. Watson, and G. Warren. 1997. Partitioning of the Golgi apparatus during mitosis in living HeLa cells. *J. Cell Biol.* 137:1211–1228.

Shima, D.T., N. Cabrera-Poch, R. Pepperkok, and G. Warren. 1998. An ordered inheritance strategy for the Golgi apparatus: visualization of mitotic disassembly reveals a role for the mitotic spindle. *J. Cell Biol.* 141:955–966.

Stuart, R.A., D. Mackay, J. Adamczewski, and G. Warren. 1993. Inhibition of intra-Golgi transport *in vitro* by mitotic kinase. *J. Biol. Chem.* 268:4050–4054.

Takenaka, K., Y. Gotoh, and E. Nishida. 1997. MAP kinase is required for the spindle assembly checkpoint but is dispensable for the normal M phase entry and exit in *Xenopus* egg cell cycle extracts. *J. Cell Biol.* 136:1091–1097.

Warren, G. 1993. Membrane partitioning during cell division. *Annu. Rev. Biochem.* 62:323–348.

Warren, G., and W. Wickner. 1996. Organelle inheritance. *Cell.* 84:395–400.

Wright, J.H., E. Munar, D.R. Jameson, P.R. Andreassen, R.L. Margolis, R. Seger, and E.G. Krebs. 1999. Mitogen-activated protein kinase kinase activity is required for the G(2)/M transition of the cell cycle in mammalian fibroblasts. *Proc. Natl. Acad. Sci. USA.* 96:11335–11340.

Zaal, K.J.M., C.L. Smith, R.S. Polishchuk, N. Altan, N.B. Cole, J. Ellenberg, K. Hirschberg, J.F. Presley, T.H. Roberts, E. Siggia, et al. 1999. Golgi membranes are absorbed into and reemerge from the ER during mitosis. *Cell.* 99: 589–601.